Hydrogenic retention of high-*Z* refractory metals exposed to ITER divertor-relevant plasma conditions

2010 Nucl. Fusion 50 055004

(http://iopscience.iop.org/0029-5515/50/5/055004)

IOP Publishing and International Atomic Energy Agency Nuclear Fusion
Nucl. Fusion **50** (2010) 055004 (9pp) doi:10.1088/0029-5515/50/5/055004

Hydrogenic retention of high-Z refractory metals exposed to ITER divertor-relevant plasma conditions

G.M. Wright[1,2,a], E. Alves[3], L.C. Alves[3], N.P. Barradas[3], P.A. Carvalho[4,5], R. Mateus[4] and J. Rapp[1,6]

[1] FOM-Institute for Plasma Physics Rijnhuizen, EURATOM-FOM, Trilateral Euregio Cluster, Nieuwegein, the Netherlands
[2] MIT Plasma Science and Fusion Center, 77 Massachusetts Ave, Cambridge, MA, USA, 02139
[3] Instituto Tecnológico e Nuclear, E.N. 10, Sacavém2686-93, Portugal
[4] Associação Euratom/IST, Instituto de Plasmas e Fusão Nuclear, Instituto Superior Técnico, Av. Rovisco Pais, 1049-001 Lisboa, Portugal
[5] ICEMS, Departamento de Engenharia de Materiais, Instituto Superior Técnico, Av. Rovisco Pais, 1049-001 Lisboa, Portugal
[6] Insitute for Energy Research, FZ-Juelich, Association EURATOM, Trilateral Euregio Cluster, D-52425, Juelich, Germany

E-mail: wright@psfc.mit.edu

Received 10 December 2009, accepted for publication 19 April 2010
Published 4 May 2010
Online at stacks.iop.org/NF/50/055004

Abstract
Tungsten (W) and molybdenum (Mo) targets are exposed to the plasma conditions expected at the strike point of a detached ITER divertor ($n_e \sim 10^{20}\,m^{-3}$, $T_e \sim 2\,eV$) in the linear plasma device Pilot-PSI. The peak surface temperatures of the targets are ~1600 K for W and ~1100 K for Mo. The surface temperatures and plasma flux densities decrease radially towards the edges of the target due to the Gaussian distribution of electron density (n_e) and temperature (T_e) in the plasma column. A 2D spatial scan of the W and Mo targets using nuclear reaction analysis (NRA) shows D retention is strongly influenced by surface temperature in the range 800–1600 K and this dependence dominates over any plasma flux dependence. NRA and thermal desorption spectroscopy (TDS) show no clear dependence of retention on incident plasma fluence for the W targets with retained fractions ranging from 10^{-8}–10^{-5} $D_{retained}/D_{incident}$. NRA and TDS for the Mo targets show retention rates a factor of 4–5 higher than the W targets and this is likely due to the lower surface temperatures for the Mo plasma exposures. NRA also reveals a thin boron layer on the Mo targets but the presence of boron does not correspond to a significant increase in D retention. Overall hydrogenic retention in W and Mo is shown to be low ($D_{retained} = 10^{19}$–$10^{20}\,D\,m^{-2}$) despite exposure to high plasma flux densities (~$10^{24}\,D\,m^{-2}\,s^{-1}$). This is likely due to the elevated surface temperature due to plasma thermal loading during exposure.

PACS numbers: 52.40.Hf, 28.52.Fa, 28.52.Cx, 78.40.Kc

1. Introduction

Hydrogenic retention in the walls of ITER can affect density control and fuelling rates. Also, during deuterium(D)–tritium(T) operation, there is a safety issue as only 700 g of mobilizable T are allowed to be stored in the ITER wall. Tungsten (W), a high-Z refractory metal, is marked for use as a plasma-facing components (PFCs) material in the ITER divertor. The thermal properties of W allow it to survive the expected heat loads at the ITER strike points. Perhaps more importantly, W also has low hydrogenic solubility and, in the absence of a strong hydrogenic trap production mechanism, is expected to have low hydrogenic retention levels. Molybdenum (Mo) shares many of the same properties as W including low hydrogenic solubility, high thermal conductance and high hydrogenic diffusion rates. Although Mo cannot be used in a burning fusion device, such as ITER, due to neutron activation concerns it is used in many current tokamaks (e.g. Alcator C-Mod, FTU, TRIAM, etc) and fusion

[a] Author to whom any correspondence should be addressed.

studies. Numerous laboratory studies have confirmed low hydrogenic retention in W [1–3] and Mo [4, 5]. From this it has been assumed that W and Mo have an advantage over carbon-based materials (i.e. graphite, CFCs) with respect to trapped fuel inventory in fusion applications. However, these laboratory studies are performed at ion flux densities that are orders of magnitude less than what is measured in current tokamaks and what is expected in ITER.

Recent studies have identified a mechanism for trap production in refractory metals that may be linked to high plasma flux densities. It has been postulated that exposure of refractory metals (W and Mo) to a high flux of low-energy (<200 eV) ions leads to a build-up of stresses in the material lattice due to the low hydrogenic solubility of these metals [3]. These stresses are relieved through deformation of the lattice and the creation of vacancies, dislocations or voids, which then represent hydrogen trapping sites. There are indications that this trap production mechanism is dependent on the incident ion flux density [3], but the relationship and how it extrapolates to ITER-relevant flux densities is not clear.

The purpose of this study is to expose polycrystalline tungsten and molybdenum samples to plasma flux densities and energies that are expected at or near the ITER divertor strikepoints. This allows the hydrogenic retention at these high flux densities ($\sim 10^{24}$ m^{-2} s^{-1}) to be measured experimentally rather than relying on extrapolations from ion beam or low-density plasma experiments. This also can demonstrate any differences in the retention properties of these two refractory metals at high plasma flux densities, which would allow for a better understanding and comparison of laboratory [1–5] and tokamak [6] retention results found in the literature.

Another important factor is the influence of surface temperature. High plasma fluxes correspond to high power fluxes. It is expected that some PFCs in the ITER divertor will operate at equilibrium surface temperatures of >1000 K. Also DEMO-type reactors will operate with gas-cooled walls with a steady-state temperature of >800 K. Thus it is also important to study retention at these high temperatures and high fluxes to better understand the retention behaviour of tungsten components in the ITER divertor and in DEMO reactor scenarios.

2. Experiment

W and Mo targets were exposed to ITER divertor-relevant deuterium plasmas in the linear plasma device Pilot-PSI. The cascaded arc plasma source used in Pilot-PSI produces high plasma densities ($\leqslant 10^{21}$ m^{-3}) at low electron temperatures ($T_e < 5$ eV) [7]. The plasma is magnetically confined with an axial B-field to a narrow column (~15 mm diameter) with the highest densities and temperatures located at the centre of the column. The plasma electron density and temperatures are measured with Thomson scattering [8]. A 1D spatial scan of the electron density and temperature across the column width for a typical plasma exposure can be seen for both the W and Mo exposures in figure 1. Each plasma shot ran for a maximum of 20 s and the n_e and T_e values are repeatable to within 10% for each shot. For targets with exposure times >20 s, multiple, sequential 20 s shots were used.

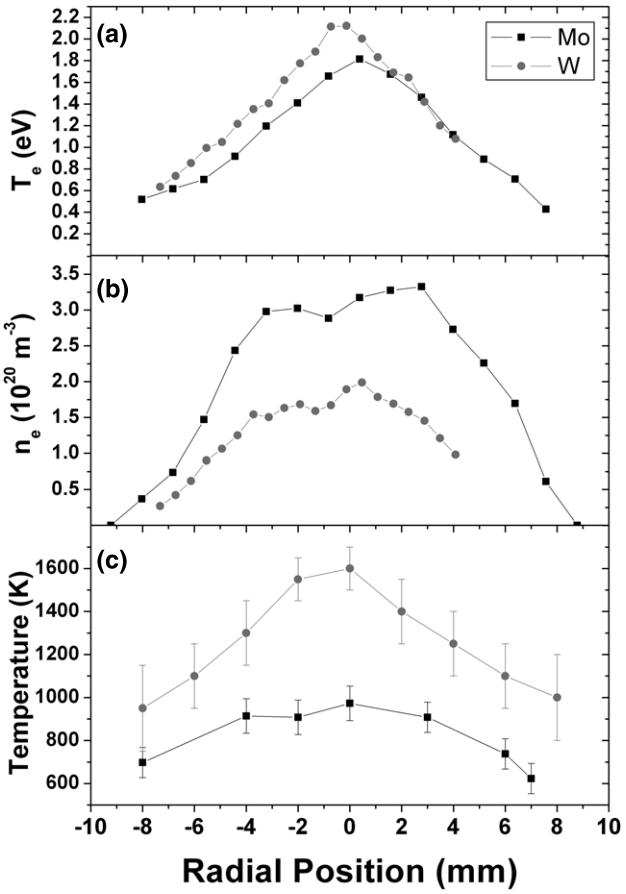

Figure 1. (*a*) Electron temperature and (*b*) electron density from a typical Thomson scattering profile in the vertical (Y) direction for the Pilot-PSI plasma column. (*c*) The surface temperature of the W and Mo targets as a function of radial position.

^{3}He NRA analysis detected the presence of boron on the surface of the exposed Mo targets. Previous exposures of Mo in Pilot-PSI have also resulted in boron deposition on the surface that likely originated from sputtering of the boron nitride spacers in the plasma source [9]. However, for the current exposures, although there is some scatter, the typical boron concentrations are a factor of ~2 less than the previous investigation [9]. No B was detected on the W targets. A difference in reflection coefficients may be the reason B deposits on a Mo surface but not on a W surface. Similar effects have been used to explain the difference of B film growth on Si, Mo and W substrates [10].

The W and Mo targets are mechanically clamped with a Mo ring to an actively cooled copper heat sink. The surface temperature was measured with a near-IR (900–1700 nm) multi-wavelength spectropyrometer. 1D surface temperature profiles can be seen for W and Mo in figure 1(*c*). Typical central surface temperatures are ~1600 K and decreasing to ~1000 K near the edges for the W targets and ~1000 K decreasing to ~700 K for the Mo targets. The lower temperatures for the Mo exposures are due to improved thermal contact between the Mo target and the heat sink due to more focused clamping pressure and the use of HI-THERM grafoil as an interface layer.

All targets are discs of 20 mm diameter (16 mm diameter exposed area). The 99.97% W polycrystalline discs were purchased from Plansee and the 99.95% Mo polycrystalline discs were purchased from Ed Fagan Inc. All targets are exposed in the 'as-received' condition (i.e. unpolished, unannealed) and were electrically grounded.

The electrical grounding of the targets can potentially affect incident ion energies and plasma fluxes. The grounding allows a net electron current to be drawn through the target. This current travels down a current channel which is approximately the size of the plasma source nozzle (in this case 10 mm diameter). Measured net currents were approximately 20 A, which is much lower than the calculated electron saturation current, which is on the order of hundreds of amperes for the measured plasma parameters in Pilot-PSI. Since electron saturation current has not been achieved, it follows that there is also a net ion current reaching the target, meaning there remains a potential drop, or sheath, in front of the target which attracts ions. With the sheath present, it remains valid to use the Bohm criterion to calculate fluxes to the target, as one would for a floating target. However, the net electron current will also induce its own potential change across this sheath region. Since the net current is measured, this potential change can be calculated using the Boltzmann factor. For a standard floating target in a hydrogen plasma, there is a standard sheath potential of $\sim 3T_e$. However, the induced current can lead to sheath potentials as low as $\sim 0.4T_e$, given the plasma parameters. This means that incident ion energies can be as low as $\sim$1 eV. All ion energies are below any sputtering or damage threshold but low energy does impact the reflection coefficient of light ions off heavy substrates. Modelling of light atom reflection indicates that reflection of D atoms off a W target ranges from 70% to 80% for $E_D < 10$ eV [11], but experiments have shown that the particle reflection can *decrease* at low energies (<100 eV) due to hydrogen (or deuterium in this case) adsorption on the surface [12] and the energy of the incoming particles approaching the chemical binding forces to the surface atoms [13]. Reflection can be a complicated process at these low energies and high particle fluxes, but it should be noted that reflection never equals unity for these situations.

The hydrogenic retention was determined with *ex situ* ion beam analysis using the ^{3}He(d,p)α nuclear reaction. For the W targets, 2.0 MeV ^{3}He ions incident to the surface yield a probing depth of $\sim 3\,\mu$m. For the Mo targets, 2.5 MeV ^{3}He ions incident to the surface yield a probing depth of $\sim 4\,\mu$m. Spectra were then analysed with the analysis program IBA DataFurnace NDF v9.2h [14] to quantify the retention. The global hydrogenic retention is determined by thermal desorption spectroscopy (TDS). The TDS was performed by clamping the targets to a ceramic heater and linearly ramping the temperature to 1273 K at a ramp rate of $\sim 1\,\mathrm{K\,s^{-1}}$ and monitoring the mass 3 (HD) and mass 4 (D_2) signals with a quadrupole mass spectrometer. Signals are calibrated and quantified with calibrated leaks of D_2 and H_2.

The microstructure of the targets was also investigated through the use of scanning electron microscopy (SEM) and transmission electron microscopy (TEM). Targets were cross-sectioned for SEM analysis with a field emission gun JEOL JSM-7001F. For TEM analysis, the targets were thinned by argon ion milling using a Gatan-Duo Mill machine operated at an acceleration voltage of 4 kV, with a 14° incident angle. TEM analysis was performed with a Hitachi H8100 instrument operated at 200 kV.

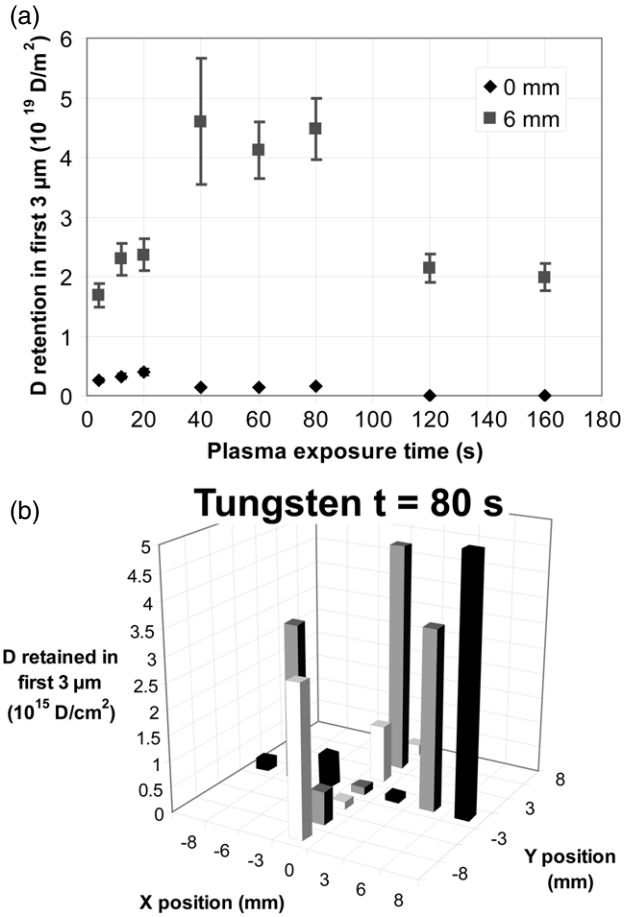

Figure 2. D retention in W as determined by NRA (*a*) as a function of plasma exposure time for the centre of the target ($T_{surf} \sim 1600$ K, $\sim 10^{24}$ D m^{-2} s^{-1}) and a point 6 mm off-centre ($T_{surf} \sim 1100$ K, $\sim 10^{23}$ D m^{-2} s^{-1}), and (*b*) in a 2D scan across target exposed for 80 s.

3. Results and discussion

3.1. d(^{3}He,p)α nuclear reaction analysis (NRA)

The NRA technique has the advantage of measuring the local concentration of D within the beam spot ($\sim$1 mm diameter) but only to the depth of the ^{3}He ion range. The NRA results were taken from various points on the target surface and each point corresponds to a different set of plasma parameters and surface temperature (see figure 1). The D retention is measured as a function of plasma exposure time which can be converted to fluence as a function of position through the plasma flux densities calculated from the Thomson scattering profile assuming the Bohm criterion (reflection *not* included).

In figure 2(*a*) the areal D retention (D m^{-2}) in the first 3 μm of the W surface is plotted as a function of plasma exposure time for the centre of the target (0 mm) and a point 6 mm off-centre. The measured retention at the centre point is very low (D concentrations $<5 \times 10^{19}$ D m^{-2}) for W despite

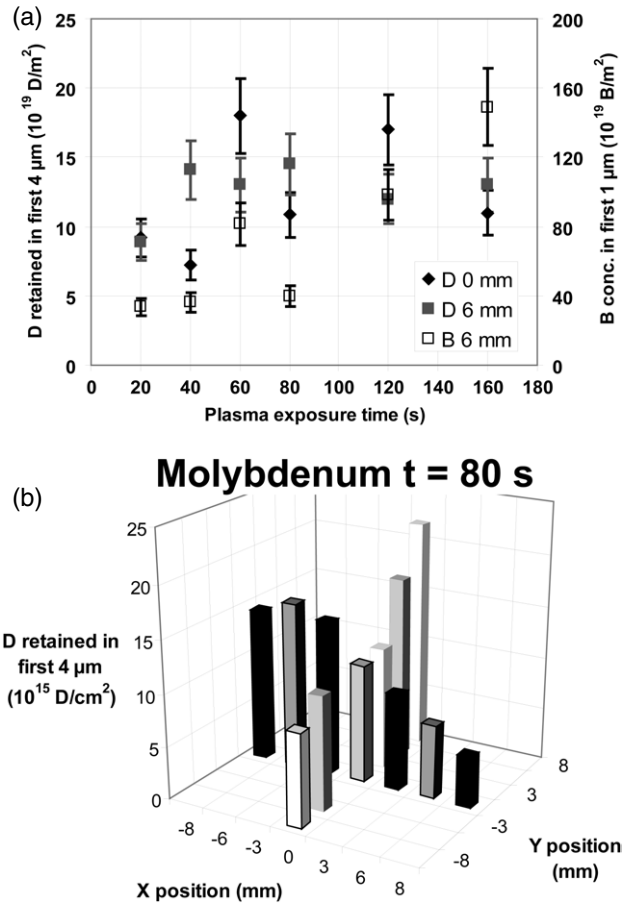

Figure 3. (*a*) D retention in M as determined by NRA as a function of plasma exposure time for the centre of the target ($T_{surf} \sim 1000$ K, $\sim 10^{24}$ D m^{-2} s^{-1}) and D retention and B deposition at a point 6 mm off-centre ($T_{surf} \sim 800$ K, $\sim 10^{23}$ D m^{-2} s^{-1}), and (*b*) a 2D scan of D retention across target exposed for 80 s, and (*b*).

the high plasma flux density ($(2.0 \pm 0.3) \times 10^{24}$ D m^{-2} s^{-1}) received in that region. The 6 mm off-centre point has a factor of 5–10 higher retention than the centre point despite being in a region exposed to lower flux densities ($(5.0 \pm 0.5) \times 10^{23}$ D m^{-2} s^{-1}) and fluences. Target surface temperature appears to be causing the difference in retention at these two locations. At the centre point the surface temperature is $\sim$1600 K and at 6 mm off-centre the temperature is $\sim$1100 K (see figure 1). A 2D NRA scan (see figure 2(*b*)) of a W target with 80 s of plasma exposure confirms that the D retention increases with radial distance from the centre in all directions. It should be noted that measurements at 8 mm off-centre are at the point where the molybdenum clamping ring overlaps with the W target, hence shadowing effects from the molybdenum ring could be responsible for the low retention measurements at some of the 8 mm off-centre points. It is well known that surface temperature plays a role in the hydrogenic retention properties of W [1, 2], thus it is likely that the lower surface temperatures in the off-centre regions are responsible for the higher D retention measured there despite this being a region of lower plasma flux and fluence since this has been qualitatively seen in other experiments [2].

In figure 3(*a*) the areal D retention in the first 4 μm of the Mo surface is plotted as a function of plasma exposure time for the centre of the target (0 mm) and a point 6 mm off-centre. The B concentration in the first 1 μm of the surface, as determined by ^{3}He NRA analysis, at the same point 6 mm off-centre is also plotted on the right-hand axis. It is assumed that the boron is deposited as a thin layer (13.1×10^{19}B/m^2 corresponds to $\sim$1 nm B layer). Here we see similar D retention at both the centre spot and 6 mm off-centre, despite the plasma fluxes at these points being $(3.0 \pm 0.4) \times 10^{24}$ D m^{-2} s^{-1} and $(9.0 \pm 1.0) \times 10^{23}$ D m^{-2} s^{-1}, respectively. The difference in plasma flux densities (and also fluence) appears to have little impact on the D retention in Mo. We can also note that while the D retention is quite similar for all exposure times, the B concentration has a large scatter. However, this scatter does not correspond with the scatter seen in the D retention. We can conclude from this that the magnitude of the B deposition is not affecting the magnitude of D retention in the Mo. This is supported by elastic recoil detection analysis (ERDA) which shows the D concentration in the B layers to range from 1.5 to 3.0 at%; meaning that there is a very small amount of total D contained within these thin B layers. However, the presence of the B may change the mechanics of the retention by modifying surface recombination or diffusion in the near-surface region. At these high temperatures, the diffusion of B into the Mo bulk is a possibility based on published diffusion rates of B in Mo [15], with typical diffusion lengths of 1–20 μm for corresponding temperatures of 700–1000 K and exposure time of 160 s. However, fits of the B peak in the NRA spectra indicate the maximum possible thickness of the B films is $\sim$500 nm, with the best fits to the data for assumed thicknesses of $\sim$50 nm or less. Even if there is a modest amount of inter-material mixing, the literature shows that small amounts of B present in Mo bulk only result in a reduction in the diffusion coefficient by a factor of 5–10 as compared with pure Mo [16]. Hence, at these exposure temperatures, it is unlikely that these thin layers of B or any modest amount of inter-material mixing would strongly inhibit D diffusion to the surface or into the bulk. Figure 3(*b*) shows the 2D NRA scan of the Mo target with 80 s of plasma exposure. This distribution shows a much more even distribution of D across the Mo surface as compared with W. Again, this is likely due to the flatter surface temperature profile of the Mo targets during plasma exposure (see figure 1). For the Mo targets the surface temperature at the centre ($\sim$1000 K) only decreased $\sim$200 K to the surface temperature at a point 6 mm off-centre ($\sim$800 K), as compared with the W targets where the temperature decreased by $\sim$500 K across the same distance. Data from the literature [5, 17] also indicate that the dependence of hydrogenic retention rates on surface temperature is not as strong at temperatures in the range 800–1000 K.

The lower surface temperatures for the Mo plasma exposures also lead to overall larger D retention in the Mo targets. The retention in the Mo targets is typically a factor of 4–5 higher than measured with the W targets. It should be mentioned that the Mo targets also receive slightly higher plasma flux and fluence than the W targets, but it has already been shown in figures 2 and 3 that this does not play a strong role in determining the retention. All indications are that target surface temperature is the dominant factor in determining retention rates for these conditions. Despite varying plasma flux densities and fluences, the retention rates seem to most

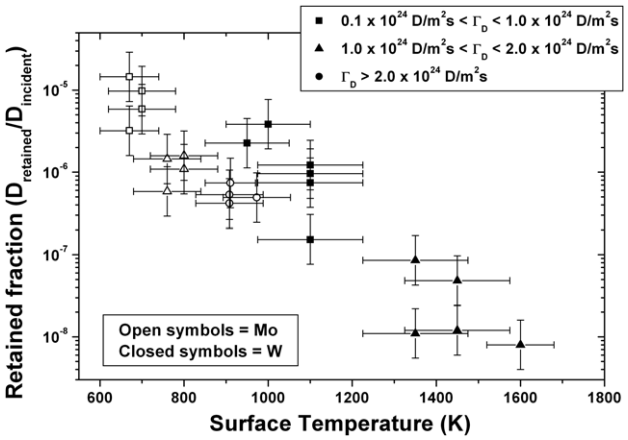

Figure 4. Retained fractions from various radial locations on W and Mo targets exposed for 80 s (see figures 2(*a*) and 3(*a*)).

closely follow surface temperature. This is clearly seen in figure 4 where the retained fraction ($D_{\text{retained}}/D^{+}_{\text{incident}}$) is plotted as a function of temperature for the data shown in figures 2(*b*) and 3(*b*). Despite a wide range of plasma flux densities, the retention exponentially decays as a function of temperature for both W and Mo. In figure 4, it appears that the Mo data set indicates lower retention than the W data set; however, given the narrow range of temperature overlap, and the significant error bars for the data points, there is not enough evidence to conclude that a difference in the retention rate for Mo and W exists.

Despite achieving flux densities 2–3 orders of magnitude higher than most laboratory experiments, the retained fractions appear to be in good agreement with results found in the literature in relevant temperature ranges [5, 17–19]. These similar retention results despite significantly different plasma flux densities are further indication that plasma flux density is not playing a significant role in determining the retention properties at these surface temperatures.

3.2. Thermal desorption spectroscopy

TDS has the advantage of detecting all trapped D from the bulk and surface of the target. Unfortunately, it desorbs from all locations on the surface simultaneously, meaning the spatial origin of the desorbed D atoms are unknown. Figure 5(*a*) shows the total retained D in the W and Mo targets as a function of plasma exposure time. The incident fluence can be calculated based on an integration of the local flux density as determined by the Thomson scattering profiles (figure 1). In figure 5(*b*), the mass 4 (D_2) desorption signal is plotted as a function of temperature for the Mo and W targets with 80 s of plasma exposure.

Much like the NRA results, the TDS results show the D retention in W has no clear dependence on the incident plasma fluence as seen by the scatter in measured retention values in figure 5(*a*). The D content in Mo appears to be trending upwards as a function of fluence but may be approaching an equilibrium value at the longest exposure times. The total D content in the Mo target is a factor of ∼2–5 greater than the corresponding W target, which is consistent with the NRA data (see figures 2 and 3). The absolute value of the

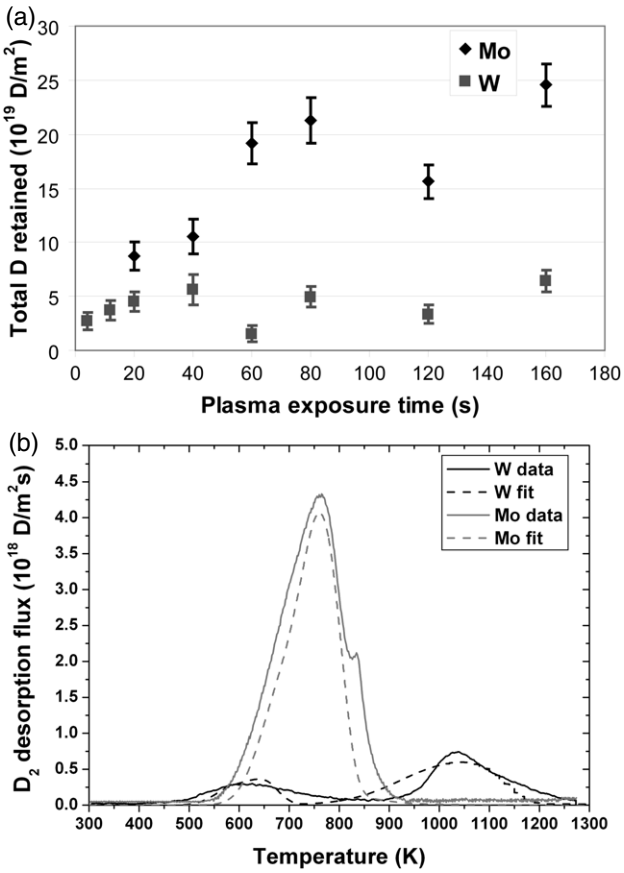

Figure 5. (*a*) The global retention as measured by TDS as a function of plasma exposure time for W and Mo, and (*b*) the D_2 desorption signal as a function of desorption temperature from W and Mo targets exposed to plasma for 80 s. Data is fit with the TMAP7 code calculations. The small peak in Mo data at ∼850 K is due to a small fluctuation in heater/temperature control during the thermal desorption.

D retention in the W and Mo is low ($<2.5 \times 10^{20}\,\text{D}\,\text{m}^{-2}$) and within the acceptable limit for tritium (T) operation in ITER (i.e. $2.5 \times 10^{20}\,\text{T}\,\text{m}^{-2} \approx 1\,\text{mg of T}\,\text{m}^{-2}$). However, when comparing NRA and TDS results it is important to take note of the differences and limitations of these techniques and how these impact the results. For NRA, D inventory is only measured in the first ∼3 μm of the surface and it is measured locally (i.e. at a specific location with a specific set of exposure conditions). Thus, NRA results contain no information for D trapped deeper than ∼3 μm in the material and it is 'blind' to retention in all non-local regions of the surface. TDS, on the other hand, gives the total retention from the entire target, meaning you measure the D retention from the entire bulk and all regions of the surface. However, this convolutes the data since it is the total integrated retention over the entire surface, which in these experiments is exposed to a wide range of plasma conditions (see figure 1). These factors could play important roles in explaining some perceived differences in the fluence dependence of the D retention seen in figures 2, 3 and 5. In figures 2 and 3, the NRA is not accounting for deep trapping, and in figure 5 a larger surface area is exposed to the cooler plasma conditions resulting in higher retention than the smaller exposed area to the high density centre of the plasma

column. This could partly explain why trends in figures 2 and 3 seem to be slightly decreasing, while trends in figure 5 seem to be increasing or flattening.

It should be noted that although plasma fluences are high when compared with other laboratory experiments, this is due to the high plasma flux densities. The exposure times are relatively short and NRA examination of the backside of the targets showed no deuterium, implying that the implanted D had not fully permeated the W target. Without full permeation of the targets, it can be assumed they are not in a state of global hydrogenic saturation since the inherent trap sites (e.g. traps introduced through fabrication and machining of the materials) distributed through the bulk of the material are not yet filled. These inherent trap sites tend to be lower energy traps [3] and thus may not contribute strongly to the retention for high-temperature plasma exposures, implying the potential for a weak dependence of retention on incident fluence. Despite no clear evidence in the data for a fluence dependence with the W targets, it is possible that the natural scatter of the data, as dictated by the semi-random distribution of these inherent trap sites, is masking a weak dependence on fluence that would only be revealed at much higher exposure times, where the target can be fully permeated by the implanted deuterium. Thus the difference between retention in a low fluence target and a fully permeated target would exceed the natural scatter in the retention data.

The mass 4 (D_2) signal from the thermal desorptions of the W and Mo targets with 80 s plasma exposure is plotted in figure 5(*b*). From the clean W target there are desorption peaks at ∼600 K and ∼1050 K with the higher temperature peak dominating the retention. For the Mo target, a single, broad desorption peak is centred at ∼750 K. With the Mo target there is no high-temperature desorption peak as is seen in the W targets. All W and Mo targets showed similar profiles to the two sample profiles in figure 5(*b*). The Mo TDS profiles had no difference in shape despite total B content varying from target to target by as much as a factor of 4, giving further indication there is not a significant amount of D trapped in the B layer as compared with the bulk Mo.

The two separated peaks seen in the TDS spectrum for W indicate multiple trap types in the tungsten, while the single peak in the Mo spectrum indicates only a single trap type responsible for the hydrogenic retention. TMAP7 [20] has been used to model the thermal desorption spectra for both W and Mo to determine the trap energies for the respective desorption peaks (see figure 5(*b*)). Diffusion and solubility values from Frauenfelder [21] and Framm [22] were used for W and Mo, respectively. Surface recombination rates are more difficult to find in the literature. For these calculations, the theoretical surface recombination rate based on sticking coefficients and solubilities described by Ogorodnikova [23] is used. A surface barrier energy (E_c) of 0.2 eV is assumed for the surface recombination coefficient of tungsten to compensate for impurities on the surface such as oxide formation, and E_c of 0.6 eV is assumed for Mo to compensate for the presence of boron on the Mo surface. Sensitivity studies have found the W results to be insensitive to the value of E_c mainly due to the generally higher surface recombination for tungsten, but Mo fits become very sensitive and difficult to fit with realistic conditions for E_c values $\geqslant$0.7 eV.

For the W targets, the desorption peaks are fit with TMAP7 using two trap energies of 1.35 ± 0.05 eV and 2.2 ± 0.1 eV. Typically, the lower trap energies signify the presence of monovacancies and dislocations in the lattice. The trap energy of 1.35 ± 0.05 eV is in good agreement with other studies that have assigned these defects a trap energy of ∼1.4 eV [3, 5, 24, 25]. The higher trap energies typically signify the presence of voids or vacancy clusters in the lattice. Previous studies have found a typical trap energy of ∼2.1 eV [5, 24, 26] for these types of defect, which is in good agreement with the fitted value of 2.2 ± 0.1 eV from the current data.

For the Mo targets, the desorption peaks are fit using a single trap energy of 1.3 ± 0.1 eV, which is in agreement with the literature for Mo [5]. The main difference between the Mo and W spectra is the apparent lack of high energy traps in the Mo targets. It should be noted that the 60 and 120 s plasma exposure for Mo targets did have a small high-temperature peak in the desorption profile, but since it was more than an order of magnitude less than the main peak, it did not significantly contribute to retention. The general lack of high energy traps in the Mo targets may be an effect of the lower surface temperature during plasma exposure. Mo irradiation studies have shown that sometimes annealing at elevated temperatures is required for void formation to occur [27, 28].

It is interesting to note that the lowest temperature desorption peaks for Mo and W occur at temperatures that are lower than the measured surface temperature of the targets during the exposures. Currently, the best explanation for the existence of these peaks is a transitional effect when the plasma is removed from the target. Due to the high rate of ion implantation and the elevated temperatures, it can be assumed that the target is saturated with D in solution, diffusing through the lattice. At the high temperatures during plasma exposure the low-energy traps ($\leqslant$1.4 eV) remain largely unpopulated. However, since the target is actively cooled, when the plasma is turned off, the target temperature returns to near room temperature in ∼1 s. As the temperature rapidly decreases, the diffusion rate of the implanted D also decreases exponentially and the time constant for these implanted D atoms to return to a surface, recombine and exit the material increases dramatically. During this time, the target temperature is now low enough that the low-energy traps can be populated. Hence it is the implanted D that has been 'frozen' in the target due to the rapid cooling after plasma exposure that populates these low-energy trap sites. This is also supported by the W TMAP7 fits where the fill fraction of the 1.35 ± 0.05 eV trap sites was set to 0.6.

3.3. Scanning and transmission electron microscopy

SEM images of target cross-sections yield valuable information on grain size and the presence of any large voids in the material. Figure 6 displays SEM images taken at the centre of the target (r = 0 mm) and at an off-centre location (r = 6 mm). The images are taken over the first ∼40 μm of the surface. The grain size at r = 0 mm is typically ∼3–5 μm, which is larger than at r = 6 mm, where the typical grain size was ∼1 μm. This is consistent with the temperature profile for the W targets where the r = 0 mm temperature is ∼1600 K and the r = 6 mm temperature is ∼1100 K and these are, respectively, above and below the recrystallization temperature of W

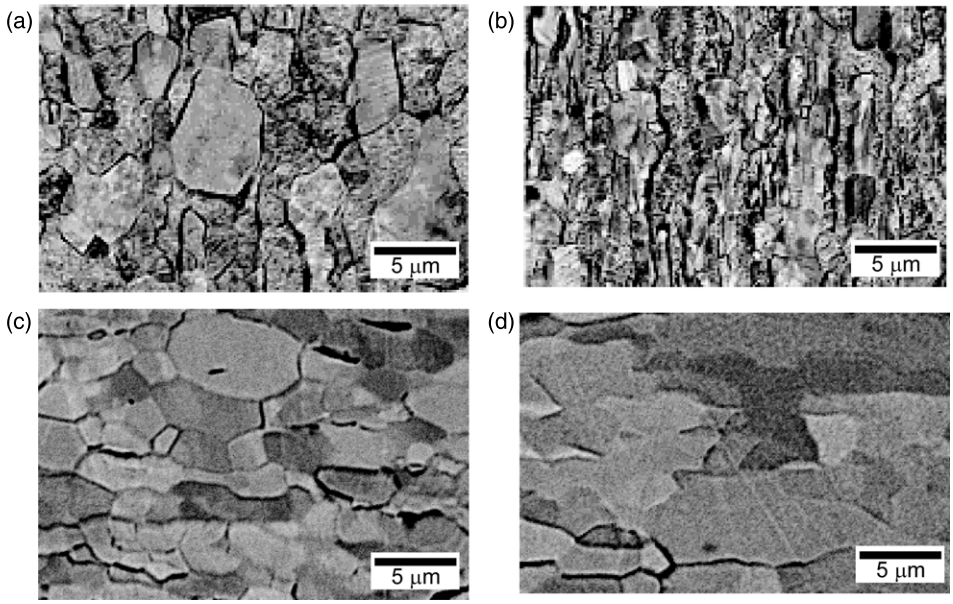

Figure 6. SEM cross-section images for (*a*) W target at 0 mm radial position, (*b*) W target at 6 mm radial position, (*c*) Mo target at 0 mm radial position and (*d*) Mo target at 6 mm radial position.

(∼1500 K). Hence the larger grains in the central portion of the target can be attributed to grain growth due to recrystallization. The dark regions seen in these SEM images are artefacts of the contrast of the image and not actual voids or cracks. Close inspection with SEM did not reveal any clear void or crack formation in the sub-surface of the W targets.

There is also significant grain growth seen in the Mo targets. The SEM analysis was only performed after TDS analysis. It is important to note that the Mo targets were heated to 1273 K for TDS, which is above the recrystallization temperature of Mo (∼1200 K). Hence, the larger grains seen in figures 6(*c*) and (*d*) are likely produced during the thermal desorptions rather than the plasma exposures where surface temperatures were measured to be below the recrystallization temperature. This is further confirmed by the fact that the large grains (∼6 μm) are seen both at the centre ($r = 0$ mm) and off-centre ($r = 6$ mm) locations of the target. There were also no voids or bubbles detected with SEM in the Mo targets.

The TEM bright-field images from the W targets revealed a mottled contrast in the grains compatible with the presence of a high density of self-interstitial dislocation loops and/or D-rich platelet clusters. However, the mottled contrast was modest and only clearly discernible close to Bragg conditions (figure 7(*a*)). This type of defects has already been reported for Mo and W irradiated with low-energy (<1 keV) D and He [29, 30]. Other defects such as nano-voids or full dislocation loops have also been seen previously in W; however, these were typically at lower irradiation temperatures [31, 32] or higher ion irradiation energies [29, 31, 32]. However, the presence of these D clusters is consistent with the TDS spectra and TMAP7 fits where the trap energy of 2.2 ± 0.1 eV can be associated with these clusters.

The TEM bright-field images from the Mo targets (figure 7(*b*)) also show a mottled contrast in grains. This contrast was even fainter than for the W targets likely indicating smaller and fewer dislocation loops and/or platelet clusters. In combination with the lack of a high-temperature desorption peak in the Mo TDS spectra, this may indicate that there is a minimum size required for the loop or cluster in order to form a high energy trap site. The reduction in the size and quantity of loops and clusters is, at least partially, due to the annealing and recrystallization the Mo undergoes during the thermal

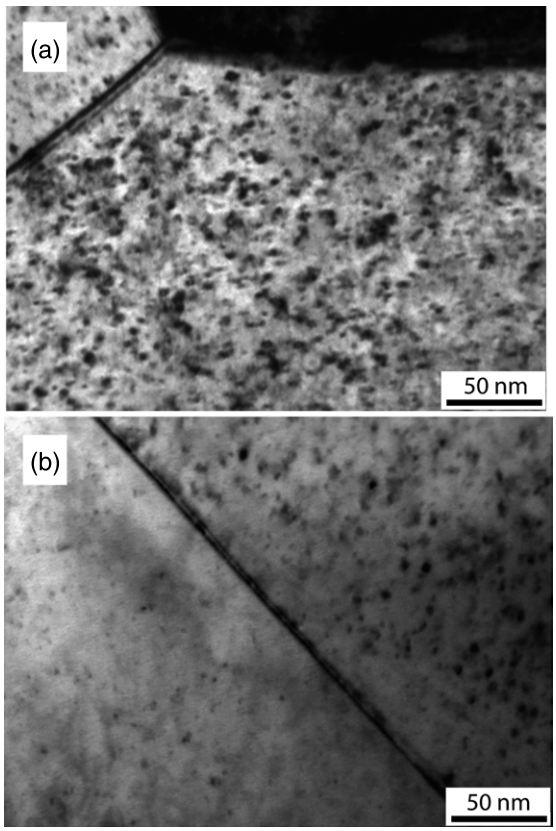

Figure 7. Bright-field TEM images close to Bragg conditions for (*a*) W targets and (*b*) Mo targets.

desorption. In Mo, dislocation loops will begin to anneal at 950 K [33] and voids and clusters will begin disassociating and annealing at 1100 K [33]. However, dissociation and annealing also take time, and since the temperature ramps for the thermal desorptions are transient at $\sim$1 K s^{-1} with a 5 min 'soak' at 1273 K and then a cooling at $\sim$3 K s^{-1}, the temperature is only $>$950 K for $\sim$12 min and $>$1100 K for $\sim$9 min. This explains why some defects can still be seen in the TEM bright-field images. In general, void and cluster annealing begins at approximately 0.35 $\times$ T_{melt} of the material; hence this defect annealing during TDS is not a concern for the W targets.

4. Conclusions

W and Mo targets have been exposed in the Pilot-PSI experiment to the plasma conditions expected at the strike point of a detached ITER divertor ($\sim 10^{24}$ m^{-2} s^{-1}, $T_{\mathrm{e}} \sim 2$ eV). The hydrogenic retention was assessed by NRA and TDS and the microstructure was investigated with SEM and TEM.

The main indication from these results is that W and Mo targets retain very little D when compared with the amount of D incident to the surface ($D_{\mathrm{retained}}/D_{\mathrm{incident}} \sim 10^{-8}$–$10^{-5}$). The W results show no clear dependence of retention on incident fluence. However, since the target has not been fully permeated by the implanted D, longer exposure times could reveal a weak dependence of retention on fluence that is currently masked by the natural scatter of the data for the short exposure times investigated here. It is concluded that the plasma exposure itself has little influence on the trapped concentrations of D in the W. The scatter in retention data for W seen in figure 2 is likely due to scatter in the population of natural or inherent defects and trap sites present in the W due to fabrication and machining, which can act as nucleation sites for D clusters or dislocation loops. It is concluded that the high surface temperature of the W during plasma exposure has mitigated the stresses formed in the high-Z lattice due to the implantation of a high flux of low energy D ions into the surface, such that new trap production is limited.

The retention in the Mo targets is higher than in W; however, this can be attributed to the lower surface temperatures during the plasma exposures of the Mo targets. Surface temperature is the dominant factor in determining retention characteristics for both Mo and W, outweighing the influence of plasma flux density and plasma fluence for the exposure conditions in this study. The presence of B on the surface of the Mo also did not seem to strongly affect the magnitude of the D retention.

Fits of the TDS spectra with TMAP7 identified trap energies of 1.35 $\pm$ 0.05 eV and 2.2 $\pm$ 0.1 eV for W and 1.3 $\pm$ 0.1 eV for Mo. These trap energies are typically associated with vacancies/dislocations and voids/clusters, respectively. TEM analysis of the W targets revealed D clusters, which likely correspond to the higher trap energies seen in the TDS spectra. The TEM for Mo targets indicated smaller and/or fewer platelet clusters, which may indicate a minimum size of clusters to form high energy trap sites.

The retention properties of Mo and W appear to be equivalent in terms of magnitude and dependence on surface temperature. Overall, the trends of retention with plasma flux and fluence observed in combination with the absolute amount of D retained when compared with the incident fluence are encouraging in terms of tritium retention in ITER. However, it should be noted that PFC neutron irradiation and lower surface temperatures could both significantly increase the hydrogenic retention in W and Mo and further work is needed in these areas.

Acknowledgments

This work, supported by the European Communities under the contract of the Association EURATOM/FOM, was carried out within the framework of the European Fusion Programme with financial support from NWO. The views and opinions expressed herein do not necessarily reflect those of the European Commission.

References

[1] Haasz A.A., Davis J.W., Poon M. and Macaulay-Newcombe R.G. 1998 *J. Nucl. Mater.* **258–263** 889
[2] Venhaus T., Causey R., Doerner R. and Abeln T. 2001 *J. Nucl. Mater.* **290–293** 505
[3] Ogorodnikova O.V., Roth J. and Mayer M. 2008 *J. Appl. Phys.* **103** 034902
[4] Haasz A.A. and Davis J.W. 1997 *J. Nucl. Mater.* **241–243** 1076
[5] Causey R.A., Kunz C.L. and Cowgill D.F. 2005 *J. Nucl. Mater.* **337–339** 600
[6] Lipschultz B. *et al* 2006 *Phys. Plasmas* **13** 056117
[7] van Rooij G.J. *et al* 2007 *Appl. Phys. Lett.* **90** 121501
[8] van der Meiden H.J. *et al* 2008 *Rev. Sci. Instrum.* **79** 013505
[9] Wright G.M. *et al* 2008 *Proc. 22nd Int. Conf. on Fusion Energy Conference 2008 (Geneva, Switzerland, 2008)* (Vienna: IAEA) CD-ROM file FT/4-2Rb, http://www-naweb.iaea.org/napc/physics/FEC/FEC2008/html/index.htm
[10] De Temmerman G. and Pitts R.A. 2008 *Fusion Eng. Des.* **83** 30
[11] Eckstein W. 1997 *J. Nucl. Mater.* **248** 1
[12] Aratari R. and Eckstein W. 1989 *Nucl. Instrum. Methods.* B **42** 11
[13] Baskes M.I. 1984 *J. Nucl. Mater.* **128** 676
[14] Barradas N.P., Jeynes C. and Webb R.P. 1997 *Appl. Phys. Lett.* **71** 291
[15] Best E. and Hinz I. 1983 *Gmelin Handbook of Inorganic Chemistry* 8th edn, Suppl. vol A3 (Berlin: Springer)
[16] Noda T. and Okada M. 1987 *Trans. Japan Inst. Met.* **28** 517
[17] Luo G.N., Shu W.M. and Nishi M. 2006 *Fusion Eng. Des.* **81** 957
[18] Tokunaga K. *et al* 2005 *J. Nucl. Mater.* **337–339** 887
[19] Causey R., Wilson K., Venhaus T. and Wampler W.R. 1999 *J. Nucl. Mater.* **266** 467
[20] Longhurst G.R. 2004 TMAP7: Tritium Migration Analysis Program, User Manual, *Idaho National Laboratory*, INEEL/EXT-04-02352
[21] Frauenfelder R. 1968 *J. Chem. Phys.* **48** 3955
[22] Fromm E. and Gebhardt E. 1976 *Gase und Kohlenstoff in Metallen* (Berlin: Springer)
[23] Ogorodnikova O.V. 2009 *J. Nucl. Mater.* **390–391** 651
[24] Poon M., Haasz A.A. and Davis J.W. 2008 *J. Nucl. Mater.* **374** 390
[25] Eleveld H. and van Veen A. 1992 *J. Nucl. Mater.* **191–194** 433
[26] van Veen A., Filius H.A., De Vries J., Bijkerk K.R., Rozing G.J. and Segers D. 1988 *J. Nucl. Mater.* **155–157** 1113
[27] Nielsen B., Hansen H.E., Nielsen H.K., Bentzon M.D. and Peterson K. 1985 *Proc. 7th Int. Conf. on Positron Annihilation, New Delhi, India 6–11 January 1985* p 497

[28] Eleveld H. and van Veen A. 1994 *J. Nucl. Mater.* **212–215** 1421
[29] Sakamoto R., Muroga T. and Yoshida N. 1994 *J. Nucl. Mater.* **212–215** 1426
[30] Iwakiri H., Yasunaga K., Morishita K. and Yoshida N. 2000 *J. Nucl. Mater.* **283–287** 1134
[31] Matsui T., Muto S. and Tanabe T. 2000 *J. Nucl. Mater.* **283–287** 1139
[32] Sakamoto R., Muroga T. and Yoshida N. 1995 *J. Nucl. Mater.* **220–222** 819
[33] Naidu S.V., Sen Gupta A., Roy R. and Sen P. 1984 *Phys. Lett.* A **101** 512